J. Plasma Physics (1999), *vol.* 62, *part* 4, *pp.* 397–423. Printed in the United Kingdom

© 1999 Cambridge University Press

Evolution of long waves and chaos in magnetohydrodynamics

ANJU PUSRI and S. K. MALIK

Department of Mathematics, Panjab University, Chandigarh-160014, India

(Received 10 September 1998 and in revised form 1 March 1999)

Abstract. The evolution equation for a wavepacket travelling on the surface of a conducting fluid of finite depth in $2+1$ dimensions in the long-wave approximation is studied in the context of magnetohydrodynamics. The amplitude equation thus obtained is the well-known Kadomtsev–Petviashvili equation with modified coefficients in the presence of a tangential magnetic field. By taking the double limit of this equation, Schrödinger–Poisson type equations are obtained. A nonlinear evolution equation is sought, in order to study Rayleigh–Taylor instability. It is shown that the magnetic field and surface tension have a stabilizing influence on the formation of bubbles arising owing to this instability. By incorporating forcing and damping terms in the Kadomtsev–Petviashvili equation, a condition for the existence of transverse homoclinic orbits giving rise to chaotic motions is obtained by using the Melnikov function method. It is shown that the chaotic motions can be suppressed by applying a suitably strong magnetic field. A study of subharmonic bifurcation leading to surface waves is also undertaken. The tangential magnetic field has a stabilizing influence on such motions.

1. Introduction

The propagation of surface waves in $2+1$ dimensions in an ideal fluid was investigated by Kadomtsev and Petviashvili (1970). The initial disturbance consists primarily of nearly one-dimensional small-amplitude long waves. They derived the evolution equation for the amplitude under the assumption that the steepness coefficient $\varepsilon(\equiv a/b) \ll 1$ with $(Kb)^2 \ll O(\varepsilon)$ and $(1/K)^2 \ll O(\varepsilon)$, where a, b and $K = (k, l)$ are the characteristic amplitude of the disturbance, the depth and the wavenumber characteristic of the disturbance respectively. Kadomtsev and Petviashvili analysed the stability of this equation with respect to long transverse perturbations, and found a soliton solution. Furthermore, they reported that the soliton is unstable with respect to such perturbations when the coefficient of the dispersion term is negative. This soliton gives rise to a wave of depression leading to a so-called 'lump solution' (Ablowitz and Clarkson 1991), which is unstable to transverse perturbations.

In the limit $(Kb)^2 \gg O(\varepsilon)$, the propagation of wavepackets on the surface of an electrically conducting fluid of uniform depth in $2+1$ dimensions in the presence of a tangential magnetic field was investigated by Pusri and Malik (1995). Here, the evolution of the wave envelope is governed by two coupled partial differential equations with cubic nonlinearity. A stability analysis reveals the existence of different regions of instability. The effect of an applied

https://doi.org/10.1017/S0022377899008004 Published online by Cambridge University Press

magnetic field is significant, and also differs for different regions of stability. 'Envelope soliton' solutions and 'waveguide' solutions of the amplitude equation have also been discussed.

To investigate the dynamics and stability of forced gravity waves, Grimshaw and Tian (1994) used a forced–damped Korteweg–de Vries (fKdV) system. The fKdV equation was transformed into Hamiltonian form, and chaotic behaviour was predicted. In this paper, we extend the analyses of Davey and Stewartson (1975). Freeman and Davey (1976) and Grimshaw and Tian (1994) to study the propagation of long waves in an ideal magnetohydrodynamic (MHD) medium in the presence of a tangential magnetic field.

In Sec. 2, we outline the basic equations and appropriate boundary conditions. To obtain asymptotic solutions, we employ the multiple-scales method (Nayfeh 1973).

In Sec. 3, we derive the evolution equation for the amplitude in the presence of a magnetic field. From this equation, we find a condition for the existence of lump solutions. These lump solutions are localized waves with algebraic tails and zero phase shift.

When the small amplitude parameter ε and the parameter $\Delta = \varepsilon/(Kb)^2$ both tend to zero, we obtain Schrödinger–Poisson-type equations in the presence of a magnetic field by considering the double limit of the amplitude equation. These equations are obtained by employing the multiple-scale averaging method in Sec. 4. These equations can be solved by the inverse scattering transform (Ablowitz and Clarkson 1991), giving a soliton solution.

In Sec. 5, we examine the evolution of the nonlinear Rayleigh–Taylor instability in the presence of a magnetic field. The Rayleigh–Taylor instability in the presence of a magnetic field was originally studied by Chandrasekhar (1961). It was also investigated by Infeld and Rowlands (1988) for ideal fluids and by Malik and Singh (1989, 1991) for ferrofluids. Using a Lagrangian extrapolation scheme to model this problem, we obtain the nonlinear evolution of the wavepacket at the free surface. We compute the time-dependent wave profile in the presence of a magnetic field. We show that this wave profile becomes multivalued for some values of a and τ, where a is the amplitude of the wave profile and τ is the time parameter. Furthermore, the fluid layer develops a loop when τ exceeds a critical breakup time τ_c. We show numerically that the formation of bubbles can be inhibited either by increasing the strength of the magnetic field or by using fluids with higher surface tension.

Abdullaev (1989) studied chaotic phenomena for gravity waves. These were also examined by Ockendon and Ockendon (1973) for the resonant forcing of water waves in a horizontal container. The analytical solutions thus obtained exhibit solitary-wave behaviour. Later, Grimshaw and Tian (1994) investigated the chaotic dynamics of the fKdV system using the Melnikov function method (Melnikov 1963) for various values of the damping parameter. In Sec. 6, we study the chaotic dynamics of the long-wave equation in $1+1$ dimensions obtained in Sec. 3, in the presence of weak damping and external periodic forcing. We first transform the amplitude equation into Hamiltonian form. The homoclinic orbits are obtained from the unperturbed, integrable Hamiltonian. For the perturbed system, periodic oscillations are found. We also discuss the non-resonant case, the primary resonance case and the secondary resonance case. The response curves show the stabilizing effect of the magnetic field on the

https://doi.org/10.1017/S0022377899008004 Published online by Cambridge University Press

system. Furthermore, we predict the various regions in parameter space where the perturbed system has transverse homoclinic orbits by constructing the appropriate Melnikov function. The existence of such orbits implies that the chaotic motions of the Smale horseshoe map occur in this forced and damped system. Subharmonic bifurcation solutions and a necessary condition for the existence of chaos are also obtained.

2. Formulation of the problem

We consider a perfectly conducting fluid bounded above by a free surface and below by a rigid surface at $z = -b$. The fluid is assumed to be homogeneous, incompressible and inviscid, with density ρ. Moreover, it is assumed to extend to infinity in the horizontal directions, so that sidewall effects can be ignored. The region above the fluid is assumed to be vacuum. We let $\mathbf{H}_0 = (H_0, 0, 0)$ be a uniform magnetic field applied along the x axis. The free surface is characterized as a surface of constant pressure. The system is also under the influence of a gravitational force $\mathbf{g} = (0, 0, -g)$.

The equations governing the system are

$$\rho\left[\frac{\partial \mathbf{u}}{\partial t} + (\mathbf{u}\cdot\boldsymbol{\nabla})\mathbf{u}\right] = -\boldsymbol{\nabla}\Pi + (\mathbf{h}\cdot\boldsymbol{\nabla})\mathbf{h} + \rho\mathbf{g}, \tag{1}$$

$$\frac{\partial \mathbf{h}}{\partial t} = (\mathbf{h}\cdot\boldsymbol{\nabla})\mathbf{u} - (\mathbf{u}\cdot\boldsymbol{\nabla})\mathbf{h}, \tag{2}$$

$$\boldsymbol{\nabla}\cdot\mathbf{u} = 0, \tag{3}$$

$$\boldsymbol{\nabla}\cdot\mathbf{h} = 0, \tag{4}$$

Here, $\mathbf{u} = (u, v, w)$ and $\mathbf{h} = (h_x, h_y, h_z)$ are the perturbations of the fluid velocity and the magnetic field respectively. $\Pi = p/\rho + \frac{1}{2}|h|^2$ is the total pressure due to the fluid and the applied magnetic field.

The relevant boundary conditions at the perturbed surface $z = \eta(x, y, t)$ are given by

$$\frac{\partial \eta}{\partial t} + (\mathbf{u}\cdot\boldsymbol{\nabla})\eta = w, \tag{5}$$

$$\mathbf{n}\cdot\mathbf{h} = \mathbf{n}\cdot\mathbf{h}_0, \tag{6}$$

$$\Pi - g\eta + T\left\{\frac{\partial^2\eta}{\partial x^2}\left[1 + \left(\frac{\partial\eta}{\partial y}\right)^2\right] + \frac{\partial^2\eta}{\partial y^2}\left[1 + \left(\frac{\partial\eta}{\partial x}\right)^2\right] - 2\frac{\partial^2\eta}{\partial x\,\partial y}\frac{\partial\eta}{\partial x}\frac{\partial\eta}{\partial y}\right\} \times\left[1 + \left(\frac{\partial\eta}{\partial x}\right)^2 + \left(\frac{\partial\eta}{\partial y}\right)^2\right]^{-3/2} - \Pi_0 = 0, \tag{7}$$

where η is the perturbation of the surface at any time t, T is the coefficient of surface tension and Π_0 is the pressure above the fluid, which is given by $\frac{1}{2}|h_0|^2$ (Pusri and Malik 1995). We consider the perturbed magnetic field above the fluid as

$$\mathbf{h}_0 = H_0\,\hat{\mathbf{e}}_x + \boldsymbol{\nabla}\Psi, \tag{8}$$

where Ψ is the perturbed magnetic potential in vacuum, satisfying, for $z > \eta(x, y, t)$,

$$\nabla^2\Psi = 0, \tag{9}$$

https://doi.org/10.1017/S0022377899008004 Published online by Cambridge University Press

The motion of the fluid vanishes at the conducting walls, implying that

$$w \to 0 \quad \text{as} \quad z \to -b, \tag{10}$$

$$h_z \to 0 \quad \text{as} \quad z \to -b, \tag{11}$$

along with

$$\frac{\partial \Psi}{\partial z} \to 0 \quad \text{as} \quad z \to -b. \tag{12}$$

In order to study the narrowband spectrum of the wavepackets in the shallow-water limit, we introduce the following dimensionless variables (Malik and Singh 1991):

$$(x, y, z) = L(\varepsilon^{-1/2}x^*, \varepsilon^{-1}y^*, z^*), \qquad t = \left(\frac{L}{\varepsilon g}\right)^{1/2} t^*, \qquad \eta = \varepsilon h \eta^*, \tag{13a–c}$$

$$\mathbf{u} = (gL)^{1/2}(\varepsilon u^*, \varepsilon^{3/2}v^*, \varepsilon^{1/2}w^*), \qquad \mathbf{h} = H_0(\varepsilon h_x^*, \varepsilon^{3/2}h_y^*, \varepsilon^{1/2}h_z^*), \tag{13d, e}$$

$$\Psi = \varepsilon^{1/2} H_0 \Psi^*, \qquad T = \rho g L T^*, \qquad \Pi = \varepsilon \rho g L \Pi^*, \qquad A_0^2 = \frac{\mu}{4\pi \rho g L} H_0^2. \tag{13f–i}$$

The asterisk indicates a non-dimensional quantity. Here ε is a small parameter representing the steepness of the wave and L denotes the characteristic horizontal length scale. The relevant dimensionless equations together with the boundary conditions corresponding to various orders are given in Appendix A.

A priori information about the elevation of the surface $\eta(x, y, t)$ is needed for the evaluation of the boundary equations (5)–(12). To circumvent this problem, we use Maclaurin series expansions for various physical quantities around $z = 0$ in terms of the small parameter ε:

$$\Phi(x, y, z, t) = \sum_{n=0}^{N} \varepsilon^n \Phi_n(x, y, z, t) + O(\varepsilon^{N+1}), \tag{14}$$

where Φ can be any of the physical quantities $\mathbf{u}$, $\mathbf{h}$, η, etc.

On substituting (14) into (A 1)–(A 4) the transformed boundary conditions (A 5)–(A 11) from Appendix A and equating powers of ε, we obtain the linear and successive nonlinear partial differential equations for various orders (see Appendix B).

In the subsequent discussion, we drop the asterisk. Making use of the pressure-balance condition (B 17) and the solutions of (B 1)–(B 21) that are $O(1)$ from Appendix B, we obtain the general wave equation corresponding to $O(\varepsilon)$:

$$\frac{\partial^2 \eta_1}{\partial t^2} - V_0^2 \frac{\partial^2 \eta_1}{\partial x^2} = 0, \tag{15}$$

where

$$V_0^2 = b\left(1 + A_0^2 + \frac{A_0^2}{b}\right), \tag{16}$$

The d'Alembert solution of (15) is given by

$$\eta_1 = Q(x - V_0 t, t) + S(x + V_0 t, t), \tag{17}$$

where Q and S are progressive waves travelling with speed V_0 along the positive and negative axes respectively.

https://doi.org/10.1017/S0022377899008004 Published online by Cambridge University Press

Without loss of generality, from now onwards, we shall consider the propagation of the unidirectional wave Q only. As the wave profile solutions Q and S never interact, S can be described in a similar manner.

3. The amplitude equation

On introducing the coordinates

$$\xi = x - V_0 t, \quad y = y, \quad \tau = \varepsilon t, \tag{18a–c}$$

we obtain an equation for the evolution of the amplitude Q:

$$2\frac{\partial Q}{\partial \tau} + a_1 Q \frac{\partial Q}{\partial \xi} + a_2 \frac{\partial^3 Q}{\partial \xi^3} + a_3 \frac{\partial v_1}{\partial y} = 0, \tag{19}$$

$$v_1 = \frac{V_0}{b}\frac{\partial}{\partial y}\int Q\, d\xi. \tag{20}$$

On differentiating (19) with respect to ξ and making use of (20), we get the equation

$$\frac{\partial}{\partial \xi}\left(2\frac{\partial Q}{\partial \tau} + a_1 Q \frac{\partial Q}{\partial \xi} + a_2 \frac{\partial^3 Q}{\partial \xi^3}\right) + a_3 \frac{\partial^2 Q}{\partial y^2} = 0, \tag{21}$$

where

$$a_1 = \frac{3V_0}{b} + \frac{3A_0^2(b^2-1)}{bV_0}, \tag{22a}$$

$$a_2 = \frac{b}{V_0}\left(\frac{bV_0^2}{3} - \frac{A_0^2 b}{3} - T\right), \tag{22b}$$

$$a_3 = \frac{b^2}{V_0^2}. \tag{22c}$$

Equation (21) is the well-known Kadomtsev–Petviashvili (KP) equation, whose coefficients depend on the magnetic field parameter A_0^2 along with capillary–gravity effects. The solution of the amplitude equation depends upon the sign of the coefficient a_2, which becomes negative for higher values of the magnetic field strength or the surface tension coefficient, whereas for gravity waves propagating in an ideal fluid without a magnetic field, a_2 is always supercritical, since $\frac{1}{3}b^2 - T > 0$. Equations (19) and (20) yield the soliton solution

$$Q = Q_{\mathrm{amp}} \operatorname{sech}^2\left\{\frac{1}{2}\frac{a_1}{a_2}\left[x + \frac{1}{a_3^{1/2}} - \left(1 + Q_{\mathrm{amp}}\frac{a_1}{3} + \frac{1^2}{a_3}\right)V_0 t\right]\right\}. \tag{23}$$

Here Q_{amp} is the amplitude of the soliton. This soliton moves with supersonic speed. For subcritical a_2, the amplitude of the solitary wave becomes negative, and its speed decreases with increasing magnetic field. This result is very interesting, since the introduction of the magnetic field changes the nature of the wave. A wave of elevation changes into a wave of depression when a strong magnetic field is applied. Such a soliton solution is referred to as a 'lump solution'; it is unstable to the transverse perturbations (Ablowitz and Clarkson 1991).

https://doi.org/10.1017/S0022377899008004 Published online by Cambridge University Press

4. Schrödinger–Poisson equations

We consider the double limit of (19) and (20) as the parameters ε and $\Delta = \varepsilon/(Kb)^2$ tend to zero. The double limit is uniform, since the order in which the limits are taken is immaterial.

We expand Q and hence (u, v) in (19) and (20) in the following series:

$$Q(\xi, \tau, y) = \varepsilon^{r_n} Q_n \exp(in\,\xi). \tag{24}$$

We introduce the scales

$$\xi_1 = \varepsilon(\xi + 3a_2\tau), \qquad t_1 = 6\varepsilon^2 a_2 \tau, \qquad \eta = \Delta y,$$

and take

$$Q_n = \Delta r_n q_n(\xi_1, \tau, y), \qquad \tilde{Q}_n = Q_{-n}, \qquad r_0 = 2. \tag{25a–c}$$

Using (24) and (25) in the KP equation (21), we obtain

$$\left[3a_2\left(\varepsilon\frac{\partial}{\partial\xi_1} + in\right) + 6\varepsilon^2 a_2 \frac{\partial}{\partial t_1}\right]\varepsilon^{r_n} Q_n + a_1\left(\varepsilon\frac{\partial}{\partial\xi_1} + in\right)\sum_m \varepsilon^{r_m + r_{n-m}} Q_m Q_{n-m}$$
$$+ a_2\left(\varepsilon\frac{\partial}{\partial\xi_1} + in\right)^3 \varepsilon^{r_n} Q_n + \varepsilon^{r_n+1}\frac{a_3}{2}\frac{\partial}{\partial\eta}(v_{10} + v_{11} + \ldots) = 0 \tag{26}$$

Particular cases of interest are when $n = 0$ and $n = 1$.

For $n = 0$, (26) reduces to

$$3a_2\frac{\partial Q_0}{\partial\xi_1} + a_1\frac{\partial|Q_1|^2}{\partial\xi_1} + \frac{a_3}{2}\frac{\partial v_{10}}{\partial\eta} = 0, \tag{27a}$$

$$\left(u_{10}, \frac{\partial v_{10}}{\partial\xi_1}\right) = \frac{V_0}{b}\left(Q_0, \frac{\partial Q_0}{\partial\eta}\right). \tag{27b}$$

For $n = 1$, (26) becomes

$$6a_2\frac{\partial Q_1}{\partial t_1} + 3ia_2\frac{\partial^2 Q_1}{\partial\xi_1^2} + ia_1(Q_2 Q_{-1} + Q_1 Q_0) + \frac{a_3}{2}\frac{\partial v_{11}}{\partial\eta} = 0, \tag{28a}$$

$$(u_{11}, iv_{11}) = \frac{V_0}{b}\left(Q_1, \frac{\partial Q_1}{\partial\eta}\right). \tag{28b}$$

On substituting for v_{11} from (28b) into (28a), we get

$$2i\frac{\partial Q_1}{\partial t_1} - \frac{\partial^2 Q_1}{\partial\xi_1^2} + \frac{V_0}{6b}\frac{a_3}{a_2}\frac{\partial^2 Q_1}{\partial\eta^2} = \frac{a_1}{3a_2}(Q_2 Q_{-1} + Q_1 Q_0). \tag{29}$$

In order to evaluate Q_0 and Q_1, we first substitute for u_{10} and v_{10} from (27b) into (27a), to get

$$\frac{\partial u_{10}}{\partial\xi_1} + \frac{a_3}{6a_2}\frac{V_0}{b}\frac{\partial v_{10}}{\partial\eta} = -\frac{a_1}{3a_2 b}\frac{\partial|Q_1|^2}{\partial\xi_1}. \tag{30}$$

This is the well-known Poisson equation. We now rearrange (27a) as

$$\frac{\partial}{\partial\xi_1}(3a_2 Q_0 + a_1|Q_1|^2) = -\frac{a_3}{2}\frac{\partial v_{10}}{\partial\eta}. \tag{31}$$

https://doi.org/10.1017/S0022377899008004 Published online by Cambridge University Press

Since ξ_1 and η are independent coordinates, each quantity on the right- and left-hand sides of (31) must be constant. Therefore Q_0 is given in terms of Q_1 by

$$Q_0 = -\frac{a_1}{3a_2}|Q_a|^2 + c, \tag{32}$$

where c is a constant of integration.

Equating powers of e^{rn} in (26) (neglecting the η_1 coordinate), we have, for a general value of n,

$$a_2(3-n^2)Q_n - a_1 \sum_m Q_m Q_{n-m} = 0. \tag{33}$$

For $n = 2$, (33) gives the value of Q_2:

$$Q_2 = \frac{a_1}{a_2}Q_1^2, \tag{34}$$

$$Q_2 Q_{-1} = \frac{a_1}{a_2}|Q_1|^2 Q_1. \tag{35}$$

We use (32) and (34) in (29), and get the following equation:

$$2i\frac{\partial Q_1}{\partial t_1} - \frac{\partial^2 Q_1}{\partial \xi_1^2} + \frac{1}{6a_2}\left(\frac{b}{V_0^2}\right)\frac{\partial^2 Q_1}{\partial \eta^2} = \frac{a_1}{3a_2}\left(\frac{a_1}{a_2}|Q_1|^2 Q_1 + \frac{b}{V_0}u_{10}Q_1\right). \tag{36}$$

Equations (36) and (30) are coupled Schrödinger–Poisson-type equations in the presence of a magnetic field. For an ideal fluid, the results of Davey and Stewartson (1974) can be obtained by putting the magnetic field parameter equal to zero. Following Ablowitz and Clarkson (1991), these equations yield a soliton solution given by

$$Q_1 = \tfrac{1}{4}K(2V_0 + K)\tanh|K(2V_0+K)|\,(x\cos\psi + y\sin\psi - Ut)\exp[i(Kx - \omega t)], \tag{37}$$

where K is a constant and $U = -K\cos\psi$; ψ is the angle that the wave groups make with the carrier wave. This represents a single depression called a negative solitary wave. It has a sharp trough, as compared with the smooth crest in a positive solitary-wave solution. It is interesting to observe that the amplitude and phase of the kink solution are sensitive to the applied magnetic field. The amplitude of the wave increase with increasing applied magnetic field.

5. Rayleigh–Taylor instability and bubble formation

The Rayleigh–Taylor instability arises when a heavy fluid is on the top of a lighter fluid. We take the upside-down configuration of the system by putting $Q \to -Q$, $S \to -S$, $g \to -g$ and $b \to -b$ in the long-wave equation obtained in Sec. 3. We have considered a straightforward treatment of the altered time dependence. Following Whitham (1974), the wave profile of the free surface Q is given by

$$Q = \alpha_1\cos(\theta)\exp(\mu\tau) + b_1^*\alpha_1^2\cos(2\theta)\exp(2\mu\tau) + b_2^*\alpha_1^3\cos(3\theta)\exp(3\mu\tau) + O(\alpha_1^4), \tag{38}$$

https://doi.org/10.1017/S0022377899008004 Published online by Cambridge University Press

where

$$b_1^* = \frac{V_0^2}{8a_2k^2}a_1', \qquad b_2^* = \frac{3V_0^2}{256a_2^2k^4}a_1'^2, \qquad a_1' = \frac{2b}{3V_0}a_1^2;$$

$$\alpha_1 = \frac{a}{b'}, \qquad \theta = k\Lambda, \qquad \alpha_1 \exp(\mu\tau) \ll 1.$$

Here a and b' are respectively the amplitude and the growth rate of the instability of the wave profile. The normalized wave speed is given as

$$\frac{\omega}{V_0 k} = 1 - \frac{a_2 k^2}{V_0} + \frac{3V_0^2 a_1'^2}{32a_2k^2}\alpha_1^2 + \ldots, \tag{39}$$

where k is the wave vector of the ripple. To incorporate nonlinear effects in the system, we introduce a Lagrangian variable γ (Infeld and Rowlands 1988) such that

$$\theta = \gamma + \alpha \sin(\gamma)\exp(\mu\tau) + \beta \sin(2\gamma)\exp(2\mu\tau), \tag{40a}$$

$$Q = (\Lambda + \alpha_1 \cos\gamma)\exp(\mu\tau). \tag{40b}$$

In order to discuss this time evolution of the surface wave profile, we incorporate the requirements that the mass be conserved for all times, such that $\bar{Q} = 0$ for every a and τ, and that the wave profile given by (40) be valid for small a.

These requirements yield

$$\Lambda = -\tfrac{1}{2}a\alpha \exp(\mu\tau), \tag{41}$$

The coefficient α, β and Λ can be determined by comparing (40a, b) with (38). Simple calculations yield

$$\Lambda = -\frac{V_0 a_1'}{8a_2k^2}, \qquad \alpha = \frac{V_0^2 a_1'^2}{4a_2k^2}\alpha_1, \qquad \beta = \frac{3V_0 a_1'^2}{128a_2^2k^4}\alpha_1^2.$$

Equations (40a, b) become multivalued for some values of τ and a. The conditions $\partial\theta/\partial\gamma = 0$ and $\partial^2\theta/\partial\gamma\,\partial\tau = 0$ give the critical value of β for sufficiently large values of the growth rate $\mu\tau$. The different parts of the interface move with different speeds, resulting in multivaluedness of Q, leading to the formation of bubbles.

The nonlinear wave profile Q has been obtained numerically by taking $a = k = 1$ and $b^2 = 3$ and by assigning various values of the non-dimensional surface tension parameter T and the magnetic field parameter A_0^2. Here the time parameter $\mu\tau$ plays an important role. For $\mu\tau = 0$, the profile is just a sine curve. As we increase the value of the normalized time $\mu\tau$, the function becomes multivalued. Figures 1(a–d) show the wave profile Q in the (Q, θ) plane when $\mu\tau = 0$, 0.75 and 1.5, for various values of the magnetic field parameter A_0^2. At $\mu\tau = 1.5$, the initial sinusoidal profile becomes steep and develops a crossover, resulting in the detachment of bubbles from the interface. When the magnetic field parameter A_0^2 and the non-dimensional surface tension parameter T are zero, we obtain a multivalued profile for $\mu\tau = 1.5$, but as we increase the value of the magnetic field, the multivalued profile returns to a sinusoidal wave profile. Interestingly, in the absence of a magnetic field, the profile is again sinusoidal for the normalized time $\mu\tau = 1.5$ and the surface tension parameter

https://doi.org/10.1017/S0022377899008004 Published online by Cambridge University Press

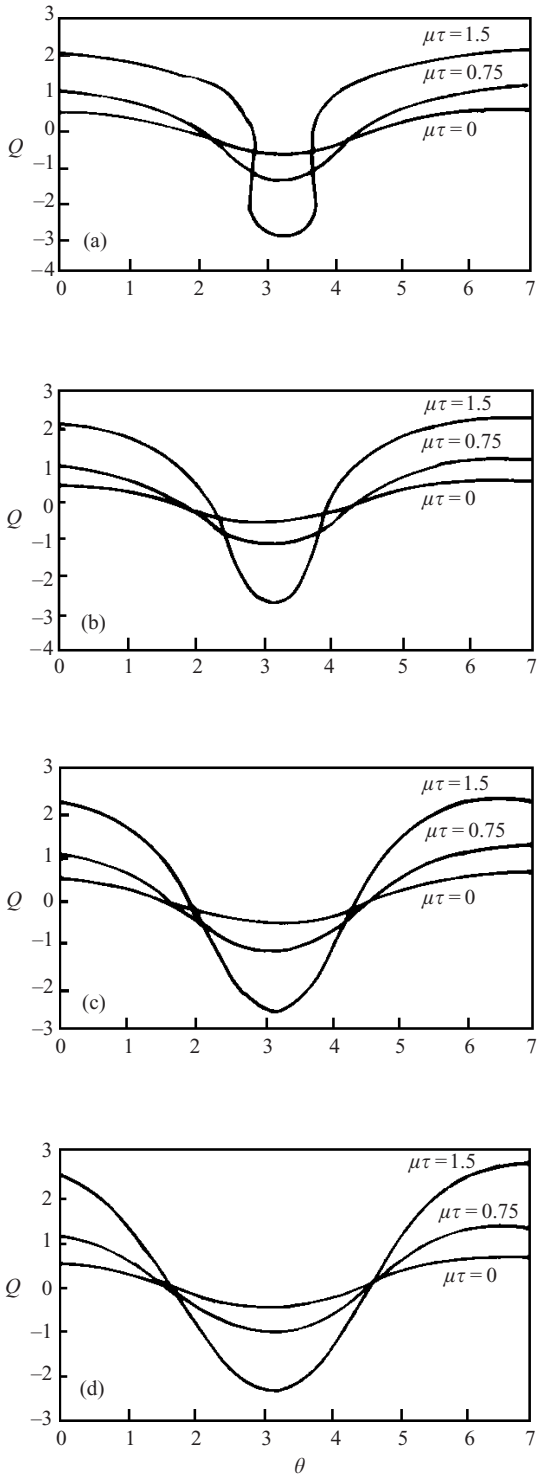


Figure 1. Interface elevation Q versus θ for the surface tension parameter $T = 0.33$, and various values of the magnetic field parameter A_0^2: (a) $A_0^2 = 0$; (b) 0.2; (c) 0.4; (d) 0.6.

https://doi.org/10.1017/S0022377899008004 Published online by Cambridge University Press

$T = 0.33$. Hence we conclude that surface tension stabilizes the system. Therefore we can prevent the formation of bubbles either by applying a higher magnetic field or by using a perfectly conducting fluid with higher surface tension.

6. Forced surface waves and chaos in MHD

In this section, we consider the propagation of surface waves on an MHD fluid that are excited by an external periodic vertical force in the presence of a steady tangential magnetic field. Sidewall effects are ignored. We now discuss parametrically excited damped long surface waves in one dimension only.

Here we take $f(\xi) = f_0 \cos(\omega\xi)$ as the external periodic forcing with period $2\pi/\omega$, where ω is the external forcing frequency of the system and ν is the damping parameter (see Grimshaw and Tian 1994). The homogeneous part of the problem admits a non-trivial solution if and only if the homogeneous part is orthogonal to every solution of the adjoint homogeneous problem. The non-secularity condition for $o(\varepsilon^2)$ yields

$$Q_\tau + \tfrac{1}{2}a_1 QQ_\xi + \tfrac{1}{2}a_2 Q_{\xi\xi\xi} + f(\xi) + \nu Q_{\xi\xi} = 0. \tag{42}$$

The coefficients a_1 and a_2 are sensitive to the applied magnetic field. Equation (42) reduces to (19) in $1+1$ dimensions if the external forcing and dissipative forces are ignored. With a view to finding a steady solution of (42), we write

$$\tfrac{1}{2}a_1 QQ_\xi + \tfrac{1}{2}a_2 Q_{\xi\xi\xi} + f(\xi) + \nu Q_{\xi\xi} = 0. \tag{43}$$

Integrating this equation with respect to ξ, we have

$$\tfrac{1}{4}a_1 Q^2 + \tfrac{1}{2}a_2 Q_{\xi\xi} + \frac{f_0}{\omega}\sin(\omega\xi) + \nu Q_\xi = c, \tag{44}$$

where c is a constant of integration.

In Sec. 3, we showed that the evolution of the amplitude in the long-wave approximation given by (19) is exactly integrable in the one-dimensional case, but the presence of forcing and damping terms complicate the situation.

6.1. Hamiltonian, homoclinic orbits and resonances

6.1.1. Case A: Zero forcing and damping. For the unperturbed system, when $f(\xi) = \nu = 0$, (44) reduces to

$$a_1 Q^2 + 2a_2 Q_{\xi\xi} = 4c. \tag{45}$$

Writing (45) as a system of equations,

$$Q_\xi = R, \tag{46a}$$

$$R_\xi = (2a_2)^{-1}(4c - a_1 Q^2), \tag{46b}$$

the Hamiltonian of the system is given by

$$H(Q,R) = (2a_2)^{-1}(\tfrac{1}{3}a_1 Q^3 - 4cQ + a_2 R^2). \tag{47}$$

The equilibrium points of this system are obtained by taking $Q_\xi = 0$ and $R_\xi = 0$ in (46a, b), and are given by

$$(Q_\pm, 0) = \left(\pm\left(\frac{4c}{a_1}\right)^{1/2}, 0\right), \qquad c \geqslant 0. \tag{48}$$

https://doi.org/10.1017/S0022377899008004 Published online by Cambridge University Press

Following Jordan and Smith (1987), we find that the system given by (46a, b) has a centre at

$$(Q_+, R) = \left(\left(\frac{4c_1}{a_1}\right)^{1/2}, 0\right)$$

and a saddle point at

$$(Q_-, R) = \left(-\left(\frac{4c_1}{a_1}\right)^{1/2}, 0\right).$$

The one-parameter family of periodic orbits in terms of Jaccobi elliptic functions (Byrd and Friedman 1971) of modulus m are given by

$$Q^m(x) = p + r\,\mathrm{cn}^2(kx), \tag{49a}$$

$$R^m(x) = -2rk\,\mathrm{sn}(kx)\,\mathrm{cn}(kx)\,\mathrm{dn}(kx), \tag{49b}$$

where sn, cn and dn are Jacobi elliptic functions of modulus m with period $T_m = 2K(m)/k$, where $K(m)$ is the complete elliptic integral of the second kind.

In order to find the constants p and r in terms of m, we make use of (47) and (49a, b). Simple calculations give

$$p = \frac{4(2m-1)}{a_1}\left[\frac{a_1 c}{4(m^2-m+1)}\right]^{1/2}, \tag{50a}$$

$$r = \frac{12m}{a_1}\left[\frac{a_1 c}{4(m^2-m+1)}\right]^{1/2} \tag{50b}$$

$$c = \frac{a_1}{4}p^2 + a_1\frac{q^2}{12m}(1-m), \tag{50c}$$

$$k = \left[\frac{a_1}{4a_2^2(m^2-m+1)}\right]^{1/4} \tag{50d}$$

$$T(m) = 4K(m)\left[\frac{a_2^2(m^2-n+1)}{4a_1 c}\right]^{1/4}. \tag{50e}$$

As $m \to 1$, the homoclinic orbits are given by

$$Q^1(\xi) = \left(\frac{4c_1}{a_1}\right)^{1/2}[1 + 3\,\mathrm{sech}^2(k\xi)], \tag{51a}$$

$$R^1(\xi) = -\frac{k}{3}\left(\frac{c}{a_1}\right)^{1/2}\mathrm{sech}^2(k\xi)\tanh(k\xi). \tag{51b}$$

6.1.2. Case B: Finite forcing and damping. In the presence of weak damping ν and an external forcing $f_0\cos(\omega\xi)$, (46a, b) take the form

$$Q_\xi = R, \tag{52a}$$

$$R_\xi = (2a_2)^{-1}\left[4c - a_1 Q^2 - 4\nu R - \frac{4f_0}{\omega}\sin(\omega\xi)\right]. \tag{52b}$$

To investigate the stability of the dynamical system (Grimshaw and Tian 1994),

https://doi.org/10.1017/S0022377899008004 Published online by Cambridge University Press

we perturb (52a, b) by a small quantity q. Consider $Q = Q_{\pm} + q$, where $Q_{\pm}$ are the equilibrium points. The presence of this perturbation modifies (52a, b) as

$$a_1 \frac{q^2}{4} + \frac{a_2}{2}\frac{\partial^2 q}{\partial \xi^2} + \nu \frac{\partial q}{\partial \xi} + \frac{f_0}{\omega}\sin(\omega\xi) + \frac{a_1}{2} Q_{\pm}\, q = 0. \tag{53}$$

There are three cases of particular physical interest that arise from (53), namely

(I) the non-resonant case, when $(a_1/a_2)Q_{\pm} \neq 0, \frac{1}{4}\omega^2, \omega^2, \frac{9}{4}\omega^2, \ldots$;
(II) primary resonance, when $(a_1/a_2)Q_{\pm} \approx \omega^2$;
(III) secondary resonance, when $(a_1/a_2)Q_{\pm} \approx \frac{1}{4}\omega^2$.

(*I*) *Non-resonant case:* $(a_1/a_2)Q_{\pm} \neq 0, \frac{1}{4}\omega^2, \omega^2, \frac{9}{4}\omega^2, \ldots$. We consider a period solution of (53) of the form $q_p = \exp(i\omega\xi)$. On substituting this periodic solution into (53) and neglecting the terms corresponding to $\exp(2i\omega\xi)$, we have

$$q_p = \mathrm{Im}\left[\frac{f_0 \exp(i\omega\xi)}{\omega^2 \mp (a_1/a_2)Q_{\pm} - i\omega\nu}\right] + O(f_0^2). \tag{54}$$

The periodic solution q_p can be rewritten as

$$q_p = R_0 \sin(\omega\xi + \phi), \tag{55}$$

$$R_0 = \frac{f_0}{[(\omega^2 \mp a_1/a_2\, Q_{\pm}) + \omega^2\nu^2]^{1/2}},$$

$$\phi = \tan^1\left[\frac{\omega\nu}{\omega^2 \mp (a_1/a_2)Q_{\pm}}\right]. \tag{55a}$$

Since Q_- is a saddle point, the perturbation is unstable, and hence q_p is unstable. For the centre Q_+, we apply perturbation theory (Jordan and Smith 1987), which predicts that q_p is stable for small values of f_0 and ν.

We led $q = q_p + \omega$ be the perturbation to the periodic solution q_p of the system given by (53). On substituting this solution into (53) and linearizing the equation by taking Q_+ instead of $Q_{\pm}$, we have

$$\omega_{\xi\xi} + \frac{2\nu}{a_2}\omega_{\xi} + \frac{a_1}{a_2}\omega(q_p + Q_+) = 0. \tag{57}$$

For the sake of simplicity, we take $\omega\xi + \phi = 2t + \frac{1}{2}\pi$. Then (55) and (57) are modified as

$$q_p = R_0 \cos(2t),$$

$$\omega_{tt} + \frac{4\nu}{a_2}\omega_t + \frac{2a_1}{a_2\omega}(q_p + Q_+) = 0.$$

The latter equation can be written as

$$\omega_{tt} + A_1\,\omega_t + A_2\,\omega(q_p + Q_+) = 0, \tag{58}$$

where

$$A_1 = \frac{4\nu}{a_2}, \qquad A_2 = \frac{4a_1}{a_2\omega}.$$

https://doi.org/10.1017/S0022377899008004 Published online by Cambridge University Press

Equation (58) is Mathieu's equation. The periodic solution is stable for $(a_1/a_2)Q_\pm \neq 0, \frac{1}{4}\omega^2, \frac{9}{4}\omega^2, \ldots$, provided that R_0 is very small.

(*II*) *Primary resonance:* $(a_1/a_2)Q_\pm \approx \omega^2$. To discuss this case, we apply the method of multiple scales (Nayfeh 1973). We introduce the scales

$$\xi = \xi_0 + \varepsilon^2 \xi_1 + O(\varepsilon^4), \tag{59a}$$

$$q = \varepsilon q_0 + \varepsilon^2 q_1 + \varepsilon^3 q_2 + O(\varepsilon^4). \tag{59b}$$

Furthermore, we assume that

$$\left| \omega^2 - \frac{a_1}{a_2} Q_\pm \right| = O(\varepsilon^2)$$

and $\nu = O(\varepsilon^2)$. We substitute (59) into (53). Introducing the operator

$$L(q_i) \equiv \frac{\partial^2 q_i}{\partial \xi_0^2} + \omega^2 q_i, \qquad i = 0, 1, 2,$$

the second-order partial differential equations at different orders are as follows:

$$O(\varepsilon): \qquad L(q_0) = 0, \tag{60}$$

$$O(\varepsilon^2): \qquad L(q_1) = -\frac{a_1}{2a_2} q_0^2, \tag{61}$$

$$O(\varepsilon^3): \qquad L(q_2) = -\frac{a_1}{a_2} q_0 q_1 - f_0 \sin(\omega\xi) - \left(\frac{a_1}{a_2} q_\pm - \omega^2 \right) q_0 - 2\frac{\partial^2 q_2}{\partial \xi_0 \partial x_1} - \frac{2\nu}{a_1} \frac{\partial q_0}{\partial \xi_0}. \tag{62}$$

The solution of (60) corresponding to $O(\varepsilon)$ is

$$q_0 = \mathscr{u} \cos(\omega\xi) + \mathscr{v} \sin(\omega\xi), \tag{63}$$

where $\mathscr{u}$ and $\mathscr{v}$ are coefficients depending upon the slower scale ξ_1. We substitute the solution of q_0 into the right-hand side of (61) and solve the differential equation for q_1. This yields

$$q_1 = \frac{a_1}{2a_2} \frac{\mathscr{u}^2 + \mathscr{v}^2}{2\omega^2} + \frac{a_1}{12a_2} \frac{\mathscr{u}^2 - \mathscr{v}^2}{\omega^2} \cos(\omega\xi) + \frac{a_1}{6a_2} \frac{\mathscr{u}\mathscr{v}}{\omega^2} \sin(\omega\xi). \tag{64}$$

On substituting the solutions of q_0 and q_1 given by (63) and (64) into (62) and following the same procedure as outlined earlier, we get the secularity conditions

$$2\omega\xi \mathscr{u}_\xi = -\frac{2\omega\mathscr{u}\nu}{a_2} + f_0 + \left(\frac{a_1}{a_2} Q_\pm - \omega^2 \right) \mathscr{v} - \frac{5}{24} \left(\frac{a_1}{a_2} \right)^2 \frac{\mathscr{u}^2 + \mathscr{v}^2}{\omega^2} \mathscr{v}, \tag{65a}$$

$$2\omega\xi \mathscr{v}_\xi = -\frac{2\omega\mathscr{v}\nu}{a_2} - \left(\frac{a_1}{a_2} Q_\pm - \omega^2 \right) \mathscr{u} + \frac{5}{24} \left(\frac{a_1}{a_2} \right)^2 \frac{\mathscr{u}^2 + \mathscr{v}^2}{\omega^2} \mathscr{u}. \tag{65b}$$

https://doi.org/10.1017/S0022377899008004 Published online by Cambridge University Press

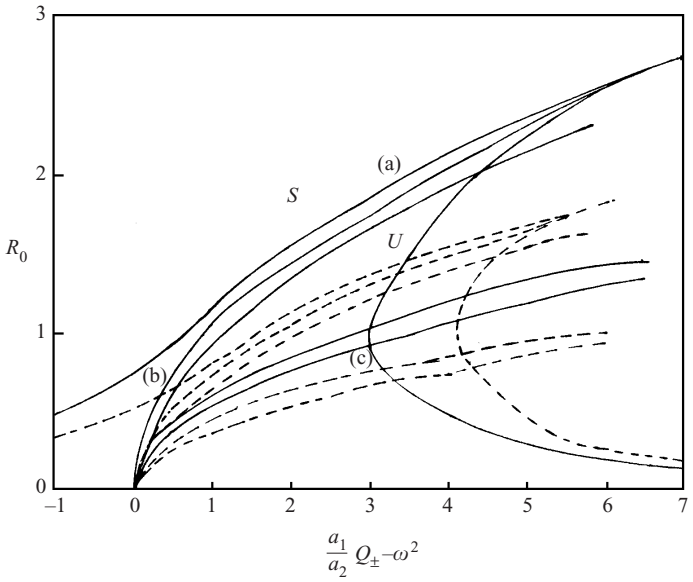


Figure 2. Stability of the response curve in the $((a_1/a_2)Q_{\pm} - \omega^2, R_0)$ plane for (a) (69) with $f_0 = \nu = 0$; (b) $(a_1/a_2)Q_{\pm} - \omega^2 = \frac{5}{24}R_0^2$, with $\nu = 0$; (c) $(a_1/a_2)Q_{\pm} - \omega^2 = \frac{15}{24}R_0^2$, with $\nu = 0$; and the instability region U representing (73) for $\nu = 1.0$. ——, $A_0^2 = 0$; – – – –, $A_0^2 = 0.6$.

Equations (65a, b) are first-order coupled differential equations. The equilibrium points $(\varkappa_0, \upsilon_0)$ of these equations are determined by taking $\varkappa_\xi = \upsilon_\xi = 0$. This condition reduces (65a, b) to the following form:

$$-\frac{2\omega\varkappa_0\nu}{a_2} + f_0 + \left(\frac{a_1}{a_2}Q_{\pm} - \omega^2\right)\upsilon_0 - \frac{5}{24}\left(\frac{a_1}{a_2}\right)^2 \frac{\varkappa_0^2 + \upsilon_0^2}{2}\upsilon_0^2 = 0, \tag{66a}$$

$$-\frac{2\omega\upsilon_0\nu}{a_2} - \left(\frac{a_1}{a_2}Q_{\pm} - \omega^2\right)\varkappa_0 + \frac{5}{24}\left(\frac{b_1}{b_2}\right)^2 \frac{\varkappa_0^2 + \upsilon_0^2}{\omega^2}\varkappa_0^2 = 0. \tag{66b}$$

We let

$$\varkappa_0 = R_0 \cos\phi_0, \qquad \upsilon_0 = R_0 \sin\phi_0.$$

Then (66a, b) are modified as follows:

$$-\frac{2\omega R_0\nu}{a_2}\cos\phi_0 + f_0 + \left(\frac{a_1}{a_2}Q_{\pm} - \omega^2\right)R_0 \sin\phi_0 - \frac{5}{24}\left(\frac{a_1}{a_2}\right)^2 \frac{R_0^3}{\omega^2}\sin\phi_0 = 0. \tag{67a}$$

$$-\frac{2\omega R_0\nu}{a_2}\sin\phi_0 - \left(\frac{a_1}{a_2}Q_{\pm} - \omega^2\right)R_0 \cos\phi_0 + \frac{5}{24}\left(\frac{a_1}{a_2}\right)^2 \frac{R_0^3}{\omega^2}\cos\phi_0 = 0. \tag{67b}$$

On multiplying (67a) by $\sin\phi_0$ and (67b) by $\cos\phi_0$, we obtain

$$R_0\left(\frac{a_1}{a_2}Q_{\pm} - \omega^2\right) + f_0 \sin\phi_0 - \frac{5}{24}\left(\frac{a_1}{a_2}\right)^2 \frac{R_0^3}{\omega^2} = 0, \tag{68a}$$

$$f_0 \cos\phi_0 - \frac{2\omega R_0\nu}{a_2} = 0. \tag{68b}$$

https://doi.org/10.1017/S0022377899008004 Published online by Cambridge University Press

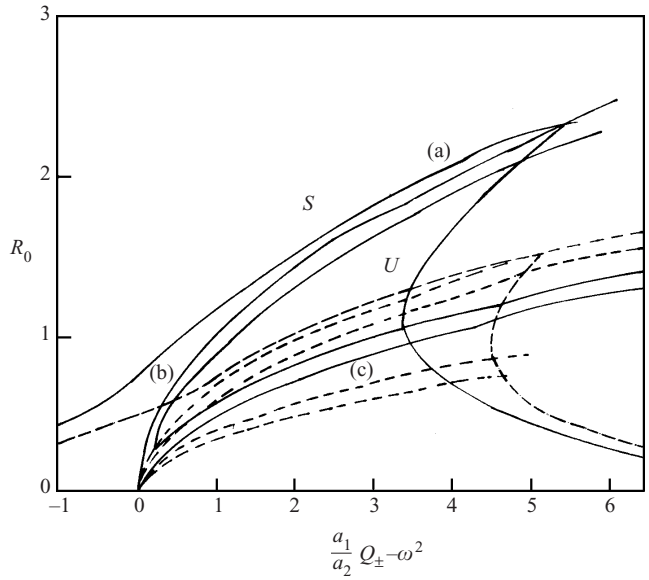


Figure 3. As Fig. 2, but for $A_0^2 = 0.2$ (——) and 0.8 (– – – –).

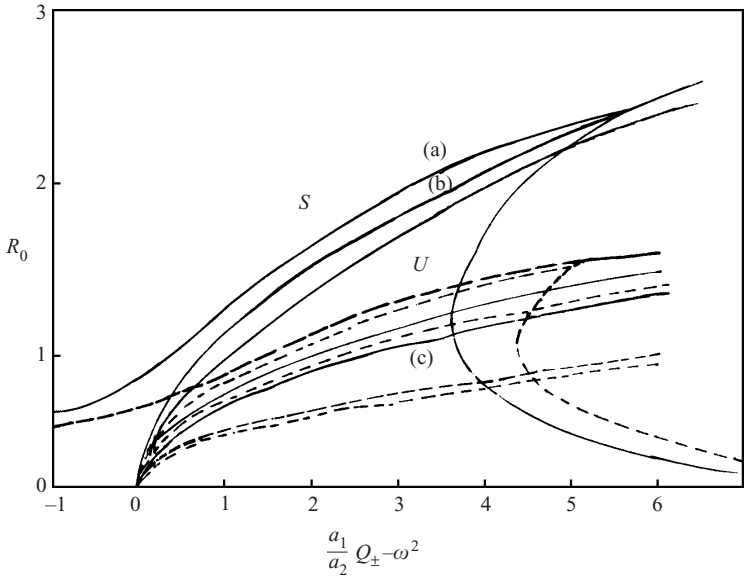


Figure 4. As Fig. 2, but for $A_0^2 = 0.4$ (——) and 1.0 (– – – –).

On eliminating ϕ_0 from (68a, b), be get

$$f_0^2 = R_0^2 \left\{ \frac{4\omega^2 \nu^2}{a_2^2} + \left[\frac{5}{24} \left(\frac{a_1}{a_2} \right)^2 \frac{R_0^2}{\omega^2} - \left(\frac{a_1}{a_2} Q_{\pm} - \omega^2 \right) \right]^2 \right\}. \tag{69}$$

Equation (69) gives the amplitude response curve. This equation may have either one or three real roots (since $R_0 > 0$), depending upon the values of the parameters ν, ω and f_0. This dependence is depicted in Figs 2–4 on the response

https://doi.org/10.1017/S0022377899008004 Published online by Cambridge University Press

diagram with various values of the magnetic field parameter A_0^2. It can be seen that with increasing magnetic field parameter, the curve (a) falls, and this results in the system being stabilized.

In order to investigate the stability of (65a, b), we perturb u and v as

$$u = \hat{u} + u_0, \qquad v = \hat{v} + v_0, \tag{70a}$$

$$\hat{u} \ll u, \qquad \hat{v} \ll v. \tag{70b}$$

By substituting u and v from (70) into (65) and linearizing the equations, a set of first-order differential equations is obtained:

$$2\omega \hat{u}_\xi = A_1 \hat{u} + B_1 \hat{v}, \tag{71a}$$

$$2\omega \hat{v}_\xi = A_2 \hat{u} + B_2 \hat{v}, \tag{71b}$$

$$A_1 = -\frac{2\omega\nu}{a_2} - \frac{5}{24}\left(\frac{a_1}{a_2}\right)^2 \frac{2u_0 v_0}{\omega^2}, \tag{72a}$$

$$B_1 = \frac{a_1}{a_2} Q_\pm - \omega^2 - \frac{5}{24}\left(\frac{a_1}{a_2}\right)^2 \frac{u_0^2 + 3v_0^2}{\omega^2}, \tag{72b}$$

$$A_2 = -\left(\frac{a_1}{a_2} Q_\pm - \omega^2\right) + \frac{5}{24}\left(\frac{a_1}{a_2}\right)^2 \frac{v_0^2 + 3u_0^2}{\omega^2}, \tag{72c}$$

$$B_2 = -\frac{2\omega\nu}{a_2} + \frac{5}{24}\left(\frac{a_1}{a_2}\right)^2 \frac{2u_0 v_0}{\omega^2}. \tag{72d}$$

Following Jordan and Smith (1987), the point (u_0, v_0) is a stable equilibrium point if

$$A_1 B_2 - B_2 A_1 > 0 \quad \text{and} \quad A_1 + B_2 \leqslant 0.$$

After some simplification, the above equations reduce the problem of stability to an eigenvalue problem with the following characteristic polynomial;

$$\left(\lambda + \frac{2\omega\nu}{a_2}\right)^2 = \left[\left(\frac{a_1}{a_2} Q_\pm - \omega^2\right) - \frac{15}{24}\left(\frac{a_1}{a_2}\right)^2 \frac{R_0^2}{\omega^2}\right]\left[\frac{5}{24}\left(\frac{a_1}{a_2}\right)^2 \frac{R_0^2}{\omega^2} - \left(\frac{a_1}{a_2} Q_\pm - \omega^2\right)\right]. \tag{73}$$

The stability and instability regions given by (73) are exhibited in Figs 2–4 for different values of the magnetic field parameter A_0^2. Curve (a) in each figure represents (69). The change of stability occurs when $\lambda = 0$ in (73). Curves (b) and (c) in each figure are parabolas when $\nu = 0$. These curves are also known as the turning points of (69). The curves corresponding to $\nu = 1$ for (73) lie between curves (b) and (c). The region between these response curves is the region of instability. This region decreases as the magnetic field strength is increased. Hence the magnetic field has a stabilizing influence on the response curves for the primary resonance case.

(*III*) *Secondary resonance:* $(a_1/a_2)Q_\pm \equiv \frac{1}{4}\omega^2$. Here we use the method of multiple scales described earlier for the case of primary resonance. Introducing the operator

$$M(q_i) \equiv \frac{\partial^2 q_i}{\partial \xi_0^2} + \frac{\omega^2}{4} q_i, \qquad i = 1, 2, 3,$$

https://doi.org/10.1017/S0022377899008004 Published online by Cambridge University Press

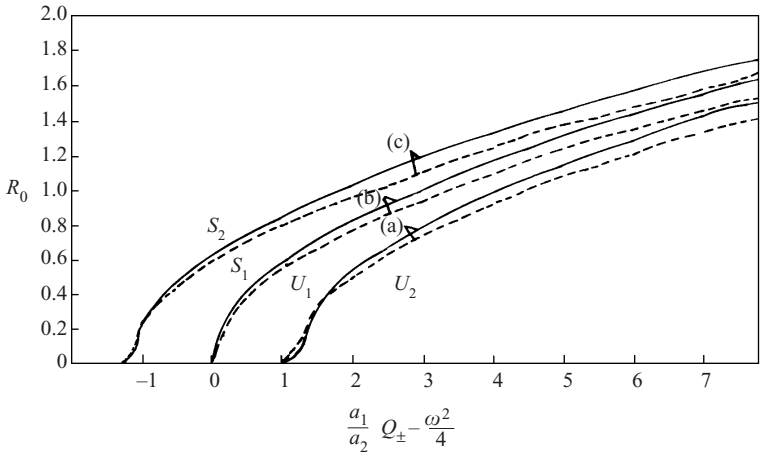


Figure 5. Diagram showing the stable regions S_1 and S_2 and the unstable regions U_1 and U_2 in the $((a_1/a_2)Q_{\pm} - \frac{1}{4}\omega^2), R_0)$ plane for (81) when (a) $\not\prec > 0$; (b) $\not\prec = 0$; (c) $\not\prec < 0$. ——, $A_0^2 = 0$; – – – –, $A_0^2 = 0.2$.

the second-order partial differential equations at different orders are as follows:

$$O(\epsilon): \quad M(q_0) = 0, \tag{74}$$

$$O(\epsilon^2): \quad M(q_1) = -\frac{a_1}{2a_2} q_0^2, \tag{75}$$

$$O(\epsilon^3): \quad M(q_3) = -\frac{a_1}{a_2} q_0 q_1 - f_0 \sin(\omega\xi) - \left(\frac{a_1}{a_2} Q_{\pm} - \frac{\omega^2}{4}\right) q_0 - 2\frac{\partial^2 q_2}{\partial\xi_0 \partial\xi_1} - \frac{2\nu}{a_2}\frac{\partial q_0}{\partial\xi_0}. \tag{76}$$

For $O(\varepsilon)$, the solution of (74) is given by

$$q_0 = \mathscr{u} \cos\left(\frac{\omega\xi}{2}\right) + \upsilon \sin\left(\frac{\omega\xi}{2}\right), \tag{77}$$

where $\mathscr{u}$ and υ are as defined earlier. The solution of (75) corresponding to $O(\epsilon^2)$ is

$$q_1 = -\frac{a_1}{a_2}\left[\frac{\mathscr{u}^2 + \upsilon^2}{\omega^2} - \frac{\mathscr{u}^2 - \upsilon^2}{\omega^2}\cos(\omega\xi) - \frac{2\mathscr{u}\upsilon}{3\omega^2}\sin(\omega\xi)\right] \tag{78}$$

Proceeding in a similar manner as before, we get the secularity condition as

$$2\omega\xi\mathscr{u}_\xi = -\frac{\omega\mathscr{u}\nu}{a_2} + f_0 + \left(\frac{a_1}{a_2} Q_{\pm} - \frac{\omega^2}{4}\right)\upsilon - \frac{5}{6}\left(\frac{a_1}{a_2}\right)^2 \frac{\mathscr{u}^2 + \upsilon^2}{\omega^2}\upsilon, \tag{79a}$$

$$2\omega\xi\upsilon_\xi = -\frac{\omega\upsilon\nu}{a^2} - \left(\frac{a_1}{a_2} Q_{\pm} - \frac{\omega^2}{4}\right)\mathscr{u} + \frac{5}{6}\left(\frac{b_1}{b_2}\right)^2 \frac{\mathscr{u}^2 + \upsilon^2}{\omega^2}\mathscr{u}. \tag{79b}$$

Equations (79a, b) are first-order coupled differential equations. The equilibrium points $(\mathscr{u}_0, \upsilon_0)$ are determined by taking $\mathscr{u}_\xi = 0$ and $\upsilon_\xi = 0$. Following the procedures as laid down earlier, we get the condition

$$\left(f_0 - \frac{2\omega\nu}{a_2}\right)\cos\phi_0 + \left[\frac{a_1}{a_2} Q_{\pm} - \frac{\omega^2}{4} - \frac{5}{6}\left(\frac{a_1}{a_2}\right)^2 \frac{R_0^2}{\omega^2}\right] R_0 \sin\phi_0 = 0, \tag{80a}$$

$$\left(f_0 - \frac{\omega\nu}{a_2}\right)\sin\phi_0 + \left[\frac{a_1}{a_2} Q_{\pm} - \frac{\omega^2}{4} - \frac{5}{6}\left(\frac{a_1}{a_2}\right)^2 \frac{R_0^2}{\omega^2}\right] R_0 \cos\phi_0 = 0. \tag{80b}$$

https://doi.org/10.1017/S0022377899008004 Published online by Cambridge University Press

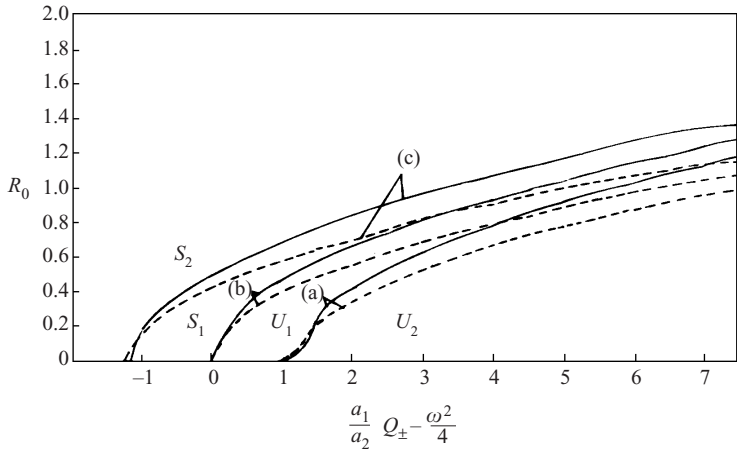


Figure 6. As Fig. 5, but for $A_0^2 = 0.4$ (——) and 0.6 (– – – –).

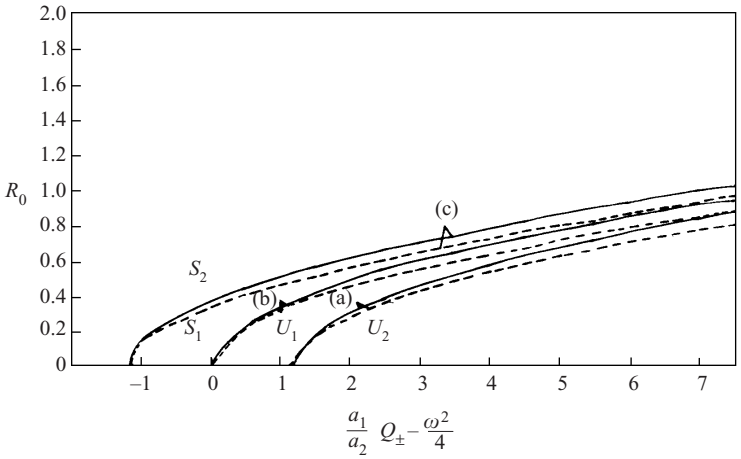


Figure 7. As Fig. 5, but for $A_0^2 = 0.8$ (——) and 1.0 (– – – –).

After some algebra, (80a, b) reduce to

$$\frac{a_1}{a_2} Q_{\pm} - \frac{\omega^2}{4} - \frac{5}{6}\left(\frac{a_1}{a_2}\right)^2 \frac{R_0^2}{\omega^2} = \not{\ell}, \tag{81}$$

where

$$\not{\ell} = \pm\left(f_0^2 - \frac{\omega^2 \nu^2}{4b^2}\right)^{1/2}. \tag{82}$$

For this case, Figs 5–7 show curves (a), (b) and (c) corresponding to (81) and (82). Curves (a), (b) and (c) represent the amplitude response curves when $\not{\ell} > 0$, $\not{\ell} = 0$ and $\not{\ell} < 0$ respectively. The region under curves (b) and (a) is the region of instability. It can be seen that as the magnetic field strength is increased, the region of instability decreases, thereby increasing the stability region.

https://doi.org/10.1017/S0022377899008004 Published online by Cambridge University Press

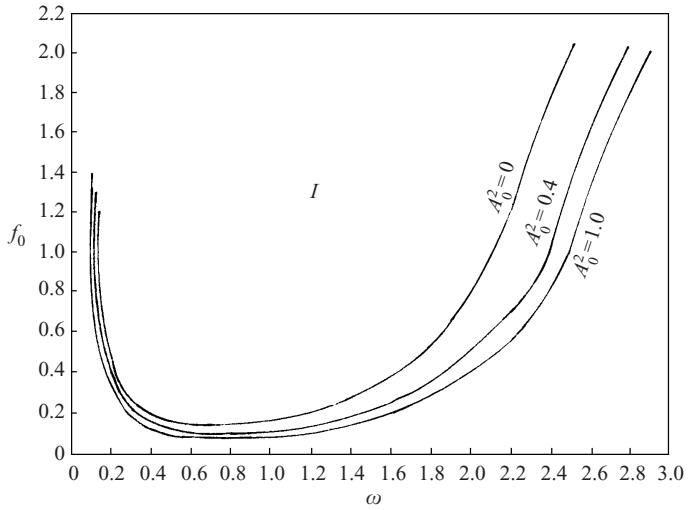


Figure 8. Diagram representing the critical surface $f_0 = (16\nu k^3 a/15\pi\omega^2)\cosh(\omega\pi/2k)$ in the (ω, ν) plane for $\nu = 0.1$ and for $A_0^2 = 0$, 0.4 and 1.0.

6.2. Chaos in a parametrically excited damped dynamical system

6.2.1. Case (i): Melnikov function method and chaos. Following Guckenheimer and Holmes (1983), we adapt the Melnikov method, which is applicable for the intersection of stable and unstable manifolds of a hyperbolic fixed point. The homoclinic Melnikov function is given by

$$M(\xi_0) = \int_{-\infty}^{\infty} f(q^\alpha(\xi - \xi_0)) \wedge g(q^\alpha(\xi - \xi_0), \xi)\, d\xi, \tag{83}$$

where

$$f = -2rk\,\mathrm{sech}^2(k\xi)\tanh(k\xi), \qquad g = -f_0\sin(\omega\xi) - \nu R$$

and ξ_0 is an initial disturbance along the original unperturbed homoclinic trajectory in the phase plane. Here ' $\wedge$ ' denotes the 'wedge product'. Substituting f and g into (83) and computing the integral, we get

$$M(\xi_0) = -\nu I_1 + 2rkf_0 I_2, \tag{84}$$

with

$$I_1 = \frac{16}{15}\nu r^2 k, \tag{85a}$$

$$I_2 = k^{-2}\left[\pi f_0 r\omega^2 \cos(\omega\xi_0)\,\mathrm{sech}\left(\frac{\omega\pi}{2k}\right)\right] \tag{85b}$$

The function $M(\xi_0)$ is the distance between the stable and unstable manifolds. From (84), the condition for the manifolds to intersect transversally (that is, where the function $M(\xi_0)$ changes sign at some ξ_0) (Guckenheimer and Holmes, 1983) is given in terms of the parameter (f_0, ω, ν) by

$$|f_0| > \frac{16k^3\nu r}{15\pi\omega^2}\cosh\left(\frac{\omega\pi}{2k}\right). \tag{86}$$

In Figs 8–10, we show plots of the critical surface

$$f = \frac{16k^3\nu r}{15\pi\omega^2}\cosh\left(\frac{\omega\pi}{2k}\right)$$

https://doi.org/10.1017/S0022377899008004 Published online by Cambridge University Press

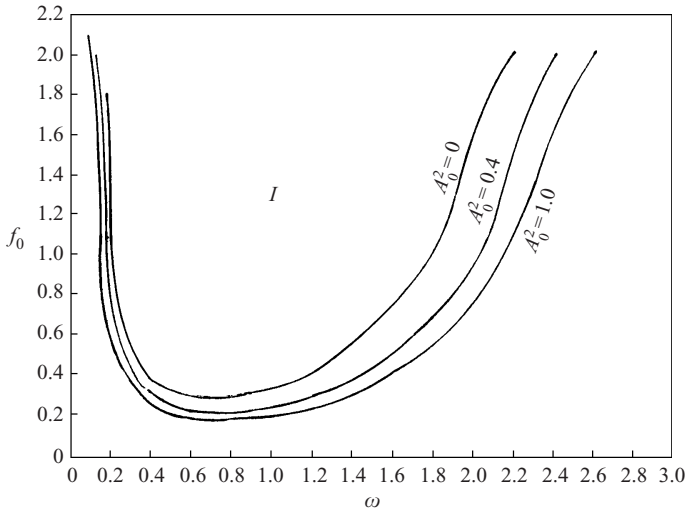


Figure 9. As Fig. 8, but for $\nu = 0.2$.

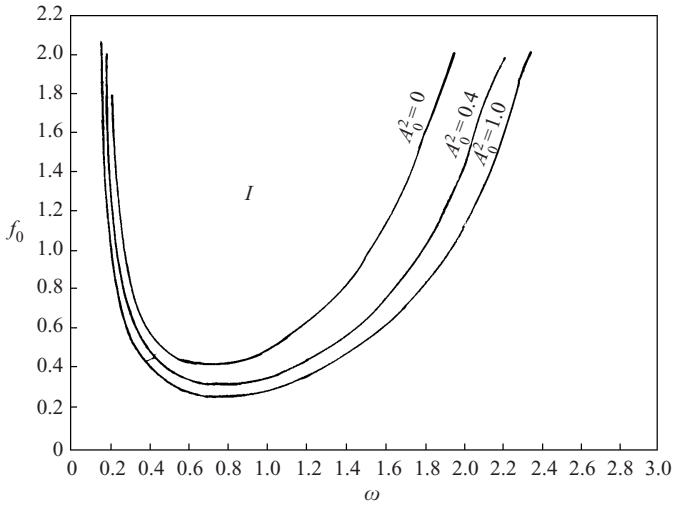


Figure 10. As Fig. 8, but for $\nu = 0.3$.

for various values of the magnetic field parameter A_0^2 in the (f_0, ω) plane for different values of the damping term ν. We find numerically that, for a fixed value of the damping parameter, an increase in the magnetic field increases the area of region I.

6.2.2. Case (ii): Subharmonic bifurcation, homoclinic tangle and chaos. We now compute the Melnikov function for resonant periodic orbits. Following Guckenheimer and Holmes (1983), the resonance condition is given by

$$4K(m)\left[\frac{a_2(m^2-m+1)}{2a_1 c}\right]^{1/4} = \frac{2\pi s}{\omega n}, \tag{87}$$

where $K(m)$ is the complete elliptic integral of the second find. For each choice

https://doi.org/10.1017/S0022377899008004 Published online by Cambridge University Press

of s and n, $m(s,n)$ can be solved uniquely from the resonant condition $T_m = sT/n$, with $T = 2\pi/\omega$. This yields a unique resonant orbit.

We compute the periodic orbit of period $T_m = sT/n$ for $m(s,n) = 1$ $(s, n \in \mathbb{Z})$, where $T = 2\pi/\omega$ is the period of the forcing term. Since there is only one centre at $(Q_{\pm}, 0)$, the periodic orbits lie only within the homoclinic orbit. Therefore the subharmonic function is given by

$$M^{s/n}(\xi_0) = \int_0^{sT} \{-\nu R^m(\xi) + R^m(\xi)\,[-f(\xi+\xi_0)]\,d\xi, \tag{88}$$

$$= \mathscr{I}_1 + \mathscr{I}_2;$$

$$\mathscr{I}_1 = -\nu P_1(m), \tag{89a}$$

$$\mathscr{I}_2 = f_0 P_2(m). \tag{89b}$$

We shall now evaluate the P_i for $i = 1, 2$:

$$P_1(m) = \int_0^{sT} 4r^2 k^2 \,\mathrm{cn}^2(k\xi)\,\mathrm{sn}^2(k\xi)\,\mathrm{dn}^2(k\xi)\,d\xi$$

$$= \int_0^{nT_m} R^2(\xi)\,d\xi,$$

$$= \int_0^{nT_m} \mathrm{cn}^2(k\xi)\,\mathrm{sn}^2(k\xi)\,\mathrm{dn}^2(k\xi)\,d\xi,$$

$$= \frac{8r^2kn}{15m^2}[2E(m) - (1-m)(2-m)K(m)], \tag{90}$$

$$P_2(m) = \int_0^{sT} \sin[\omega(\xi+\xi_0)\,R^m(\xi)\,d\xi$$

$$= -r\omega \int_0^{sT} \cos[\omega(\xi+\xi_0)]\,\mathrm{cn}^2(k\xi)\,d\xi, \tag{91}$$

where $E(m)$ and $K(m)$ are complete elliptic integrals of the second kind. The Fourier expansion of $\mathrm{cn}^2(k\xi)$ is given by

$$\mathrm{cn}^2(k\xi) = \sum_{p=0}^{\infty} b_p(m)\cos(p+1)\frac{\omega n\xi}{s}, \tag{92}$$

where

$$b_p(m) = \frac{\pi^2(p+1)}{mK^2(m)\sinh(p+1)\pi K'(m)/K(m)]}, \tag{93}$$

with $K'(m)$ the complementary elliptic modulus of $K(m)$: $K'(m) = K(1-m)$. On substituting $\omega\xi/s = y$, (19) becomes

$$P_2(m) = -rs\int_0^{2\pi} \cos(sy + \omega\xi_0) \sum_0^{\infty} b_p(m)\cos[(p+1)ny]\,dy. \tag{94}$$

Furthermore, we put $s = n(p+1)$. Then

$$P_2(m) = -rs\pi\cos(\omega\xi_0)\,b_p(m), \tag{95}$$

https://doi.org/10.1017/S0022377899008004 Published online by Cambridge University Press

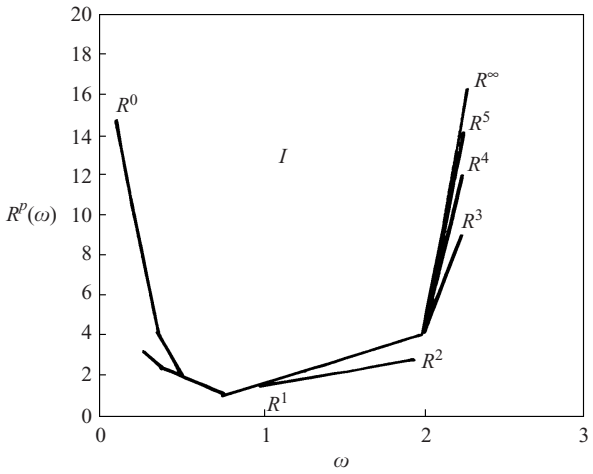


Figure 11. The subharmonic bifurcation curves R^p in the (R_p, ω) plane for $A_0 = 0$ and $p = 0, 1, 2, 3, 4, 5$ and ∞.

and hence

$$T(m) = (p+1)T. \tag{96}$$

Thus there is a sequence of periodic doubling that leads to chaos.

The Melnikov function given by (88) with the use of (90) and (95) becomes

$$\begin{aligned} M^{s/n}(\xi_0) &= M^{(p+1)}(\xi_0) \\ &= f_0 P_2(m) - \nu P_1(m), \\ &= f_0 rs\pi b_p(m)\cos(\omega\xi_0) - \frac{8r^2kn\nu}{15m^2}[2E(m) - (1-m)(2-m)K(m)], \end{aligned} \tag{97}$$

We define

$$R^p(\omega) = \frac{8rk^2}{15m^2 b_p(m) K(m)}[2E(m) - (1-m)(2-m)]. \tag{98}$$

Then we conclude from (97) that there is a pair of subharmonics of order p whenever

$$|f_0| > \nu R^p(\omega). \tag{99}$$

We have computed (99) numerically for a given set of parameter values. Figures 11 and 12 show the curves corresponding to $p = 1, 2, 3, 4, 5, \ldots$ in the plot of ω versus $R^p(\omega)$. Following Guckenheimer and Holmes (1983), it is easy to verify that as $m \to 1$ and $p \to \infty$ (by the resonance condition),

$$\lim_{m\to\infty} M^{s/n}(f_0, \omega, \nu) = M(f_0, \omega, \nu). \tag{100}$$

Figures 11 and 12 show the rate of convergence of the subharmonics given by (100). It can be seen that as the magnetic field strength increases, the region I in Figs 11 and 12 decreases. It is also observed that there is an extremely rapid convergence to the homoclinic bifurcation curve and hence chaos.

Here the homoclinic bifurcation curve is the countable limit of saddle-node bifurcation curves in a cascade of period-doubling orbits, giving rise to a Smale

https://doi.org/10.1017/S0022377899008004 Published online by Cambridge University Press

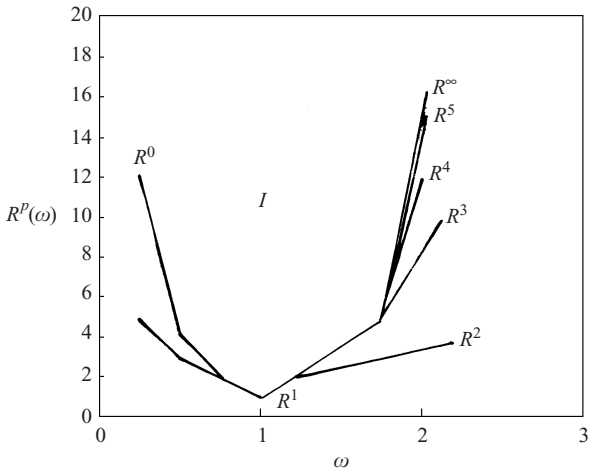


Figure 12. As Fig. 11, but for $A_0^2 = 0.2$

horseshoe and thus leading to chaotic dynamics. Note that the condition (99) for the intersection of the manifolds is independent of the particular cross-section.

7. Concluding remarks

In this paper, we have derived the well-known Kadomtsev–Petviashvili (KP) equation in the presence of a tangential magnetic field and its soliton solution. A term due to the magnetic field occurs in the soliton solution, and changes its nature for $a_2 < 0$; this is known as a 'lump solution', and is unstable to transverse perturbations.

We have then derived the Schrödinger–Poisson equation by taking the double limit of the KP equation and introducing new coordinates. Again, we have found a soliton solution of the amplitude equation. We have shown that the amplitude of the wave increases with increasing magnetic field.

We have then investigated the Rayleigh–Taylor instability in the presence of a tangential magnetic field. We have discussed this phenomenon in $1+1$ dimensions, and have shown that, owing to this instability, the wave profile becomes multivalued, resulting in the formation of bubbles. We have shown numerically that the magnetic field and the surface tension have a stabilizing influence on these bubbles.

Finally, we have incorporated a forcing and damping term into the one-dimensional KP equation. On formulating this as a Hamiltonian system we have shown the existence of homoclinic orbits. Furthermore, by making use of the Melnikov function, we have obtained conditions for the existence of chaotic motions. Numerical computations with different parameter values have shown the stabilizing effect of the magnetic field on these motions. We have also undertaken a subharmonic analysis.

https://doi.org/10.1017/S0022377899008004 Published online by Cambridge University Press

Appendix A. Dimensionless equations and boundary conditions

The dimensionless equations are

$$\frac{\partial \mathbf{u}^*}{\partial t} = -\left(\varepsilon u^* \frac{\partial}{\partial x^*} + \varepsilon^2 v^* \frac{\partial}{\partial y^*} + w^* \frac{\partial}{\partial z^*}\right)\mathbf{u}^* + A_0^2\left[(1+\varepsilon h_x^*)\frac{\partial}{\partial x^*} + \varepsilon^2 h_y^* \frac{\partial}{\partial y^*} + h_z^* \frac{\partial}{\partial z^*}\right]\mathbf{h}^* - \boldsymbol{\nabla}\Pi^*, \tag{A 1}$$

$$\frac{\partial \mathbf{h}^*}{\partial t} = -\left(\varepsilon h_x^* \frac{\partial}{\partial x^*} + \varepsilon^2 h_y^* \frac{\partial}{\partial y^*} + h_z^* \frac{\partial}{\partial z^*}\right)\mathbf{u}^* - \left(\varepsilon u^* \frac{\partial}{\partial x^*} + \varepsilon^2 v^* \frac{\partial}{\partial y^*} + w^* \frac{\partial}{\partial y^*}\right)\mathbf{h}^* + \frac{\partial \mathbf{u}^*}{\partial x^*}, \tag{A 2}$$

$$\varepsilon \frac{\partial u^*}{\partial x^*} + \varepsilon^2 \frac{\partial v^*}{\partial y^*} + \frac{\partial w^*}{\partial z^*} = 0, \tag{A 3}$$

$$\varepsilon \frac{\partial h_x^*}{\partial x^*} + \varepsilon^2 \frac{\partial h_y^*}{\partial y^*} + \frac{\partial h_z^*}{\partial z^*} = 0. \tag{A 4}$$

The boundary conditions at $z^* = \eta^*(x, y, t)$ are

$$\varepsilon \frac{\partial \eta^*}{\partial t} + \varepsilon^2 u^* \frac{\partial \eta^*}{\partial x^*} + \varepsilon^3 v^* \frac{\partial \eta^*}{\partial y^*} - w^* = 0, \tag{A 5}$$

$$h_z^* - \frac{\partial \Psi^*}{\partial z^*} = \varepsilon^2 \frac{\partial \eta^*}{\partial x^*}\left(h_x^* - \frac{\partial \Psi^*}{\partial x^*}\right) + \varepsilon^3 \frac{\partial \eta^*}{\partial y^*}\left(h_y^* - \frac{\partial \Psi^*}{\partial y^*}\right), \tag{A 6}$$

$$\varepsilon\Pi^* - \varepsilon\eta^* + \varepsilon^2 T^*\left(\frac{\partial^2}{\partial x^{*2}} + \varepsilon\frac{\partial^2}{\partial y^{*2}}\right)\left[1 + \varepsilon^3\left(\frac{\partial \eta^*}{\partial x^*}\right)^2 + \varepsilon^4\left(\frac{\partial \eta^*}{\partial y^*}\right)^2\right]\eta^* - \frac{A_0^2}{2}\left\{1 + \varepsilon\left[2\frac{\partial \Psi^*}{\partial x^*} + \varepsilon\left(\frac{\partial \Psi^*}{\partial x^*}\right)^2\right] + \varepsilon\left(\frac{\partial \Psi^*}{\partial z^*}\right)^2 + \varepsilon^3\left(\frac{\partial \Psi^*}{\partial y^*}\right)^2\right\} = 0, \tag{A 7}$$

$$\left(\varepsilon\frac{\partial^2}{\partial x^{*2}} + \varepsilon^2\frac{\partial^2}{\partial y^{*2}} + \varepsilon^3\frac{\partial^2}{\partial z^{*2}}\right)\Psi^* = 0, \tag{A 8}$$

$$w^* \to 0 \quad \text{as} \quad z \to -b, \tag{A 9}$$

$$h_z^* \to 0 \quad \text{as} \quad z \to -b, \tag{A 10}$$

$$\frac{\partial \Psi^*}{\partial z^*} \to 0 \quad \text{as} \quad z \to \infty. \tag{A 11}$$

Appendix B. The equations of motion and the boundary conditions at various orders

In the following,

$$\mathbf{u}_n = (u_n, v_n, w_n), \qquad \mathbf{h}_n = (h_{x_n}, h_{y_n}, h_{z_n}), \qquad n = 1, 2, \ldots, N.$$

https://doi.org/10.1017/S0022377899008004 Published online by Cambridge University Press

At $O(1)$, the equations are

$$\frac{\partial \mathbf{u}_1}{\partial t}+\nabla\Pi_1-A_0^2\frac{\partial \mathbf{h}_1}{\partial x}=A_0^2 h_{z_1}\frac{\partial \mathbf{h}_1}{\partial z}-w_1\frac{\partial \mathbf{u}_1}{\partial z}, \tag{B 1}$$

$$\frac{\partial \mathbf{h}_1}{\partial t}-\frac{\partial \mathbf{u}_1}{\partial x}=h_{z_1}\frac{\partial \mathbf{u}}{\partial z}-w_1\frac{\partial \mathbf{h}_1}{\partial z}, \tag{B 2}$$

$$\frac{\partial w_1}{\partial z}=0, \tag{B 3}$$

$$\frac{\partial h_{z_1}}{\partial z}=0, \tag{B 4}$$

with the boundary conditions

$$h_{z_1}-\frac{\partial \Psi_1}{\partial z}=0 \quad \text{at } z=0, \tag{B 5}$$

$$w_1=0 \quad \text{at } z=0, \tag{B 6}$$

$$w_1\to 0 \quad \text{as } z\to -b, \tag{B 7}$$

$$\frac{\partial^2\Psi_1}{\partial z^2}=0 \quad \text{as } z\to\infty, \tag{B 8}$$

$$\frac{\partial \Psi_1}{\partial z}=0, \tag{B 9}$$

$$h_{z_1}\to 0 \quad \text{as } z\to -b. \tag{B 10}$$

At $O(\varepsilon)$, the equations are

$$\frac{\partial \mathbf{u}_2}{\partial t_1}+\nabla\Pi_2-A_0^2\frac{\partial \mathbf{h}_2}{\partial x}=A_0^2 h_{x_1}\frac{\partial \mathbf{h}_1}{\partial x}-u_1\frac{\partial \mathbf{u}_1}{\partial x}. \tag{B 11}$$

$$\frac{\partial \mathbf{h}_2}{\partial t}-\frac{\partial \mathbf{u}_2}{\partial x}=h_{x_1}\frac{\partial \mathbf{u}_1}{\partial x}-u_1\frac{\partial \mathbf{h}_1}{\partial x}, \tag{B 12}$$

$$\frac{\partial u_1}{\partial x}+\frac{\partial w_2}{\partial z}=0, \tag{B 13}$$

$$\frac{\partial h_{x_1}}{\partial x}+\frac{\partial h_{z_2}}{\partial z}=0, \tag{B 14}$$

with the boundary conditions

$$\frac{\partial \eta_1}{\partial t}-w_2=0 \quad \text{at } z=0, \tag{B 15}$$

$$h_{z_2}-\frac{\partial \Psi_2}{\partial z}=0 \quad \text{at } z=0, \tag{B 16}$$

https://doi.org/10.1017/S0022377899008004 Published online by Cambridge University Press

$$\Pi_1-\eta_1-A^2\frac{\partial \Psi_1}{\partial x}=0 \quad \text{at } z=0, \tag{B 17}$$

$$\frac{\partial^2 \Psi_1}{\partial x^2}+\frac{\partial^2 \Psi_2}{\partial z^2}=0, \tag{B 18}$$

$$w_2\to 0 \quad \text{as } z\to -b, \tag{B 19}$$

$$h_{z_2}\to 0 \quad \text{as } z\to -b, \tag{B 20}$$

$$\frac{\partial \Psi_2}{\partial z}=0 \quad \text{as } z\to \infty. \tag{B 21}$$

At $O(\varepsilon^2)$, the equations are

$$\frac{\partial \mathbf{u}_3}{\partial t}+\boldsymbol{\nabla}\Pi_3-A_0^2\frac{\partial \mathbf{h}_3}{\partial x}=A_0^2\left(h_{x_1}\frac{\partial \mathbf{h}_2}{\partial x}+h_{x_2}\frac{\partial \mathbf{h}_1}{\partial x}+h_{y_1}\frac{\partial \mathbf{h}_1}{\partial y}+h_{z_1}\frac{\partial \mathbf{h}_3}{\partial z}+h_{z_2}\frac{\partial \mathbf{h}_2}{\partial z}+h_{z_1}\frac{\partial \mathbf{h}_1}{\partial z}\right)$$
$$-\left(u_1\frac{\partial \mathbf{u}_2}{\partial x}+u_2\frac{\partial \mathbf{u}_1}{\partial x}+v_1\frac{\partial \mathbf{u}_1}{\partial y}+w_1\frac{\partial \mathbf{u}_3}{\partial z}+w_2\frac{\partial \mathbf{u}_2}{\partial z}+w_3\frac{\partial \mathbf{u}_1}{\partial z}\right) \tag{B 22}$$

$$\frac{\partial \mathbf{h}_3}{\partial t}-\frac{\partial \mathbf{u}_3}{\partial x}=h_{x_1}\frac{\partial \mathbf{u}_2}{\partial x}+h_{x_2}\frac{\partial \mathbf{u}_1}{\partial x}+h_{y_1}\frac{\partial \mathbf{u}_1}{\partial y}+h_{z_1}\frac{\partial \mathbf{u}_3}{\partial z}+h_{z_2}\frac{\partial \mathbf{u}_2}{\partial z}+h_{z_1}\frac{\partial \mathbf{u}_1}{\partial z}$$
$$-\left(u_1\frac{\partial \mathbf{h}_2}{\partial x}+u_2\frac{\partial \mathbf{h}_1}{\partial x}+v_1\frac{\partial \mathbf{h}_1}{\partial y}+w_1\frac{\partial \mathbf{h}_3}{\partial z}+w_2\frac{\partial \mathbf{h}_2}{\partial z}+w_3\frac{\partial \mathbf{h}_1}{\partial z}\right), \tag{B 23}$$

$$\frac{\partial \mathbf{u}_2}{\partial x}+\frac{\partial \mathbf{v}_1}{\partial y}+\frac{\partial \mathbf{w}_3}{\partial z}=0, \tag{B 24}$$

$$\frac{\partial h_{x_2}}{\partial x}+\frac{\partial h_{y_1}}{\partial y}+\frac{\partial h_{z_3}}{\partial z}=0. \tag{B 25}$$

with the boundary conditions

$$\frac{\partial \eta_2}{\partial t}-w_3+u_1\frac{\partial \eta_1}{\partial x}+w_2\frac{\partial \eta_1}{\partial z}+w_1\frac{\partial \eta_2}{\partial z}=0 \quad \text{at } z=0, \tag{B 26}$$

$$h_{z_3}-\frac{\partial \Psi_3}{\partial z}=\frac{\partial \eta_1}{\partial x}\left(h_{x_1}-\frac{\partial \Psi_1}{\partial x}\right)-\eta_1\frac{\partial}{\partial z}\left(h_{z_2}-\frac{\partial \Psi_2}{\partial z}\right)-\eta_2\frac{\partial}{\partial z}\left(h_{z_1}-\frac{\partial \Psi_1}{\partial z}\right)=0, \tag{B 27}$$

$$\Pi_2-\eta_2+\eta_1\frac{\partial \Pi_1}{\partial z}+T\frac{\partial^2 \eta_1}{\partial x^2}-A_0^2\left[\frac{1}{2}\left(\frac{\partial \Psi_1}{\partial x}\right)^2+\frac{\partial \Psi_1}{\partial z}\frac{\partial \Psi_2}{\partial z}\right]=0 \quad \text{at } z=0, \tag{B 28}$$

$$\frac{\partial^2 \Psi_2}{\partial x^2}+\frac{\partial^2 \Psi_1}{\partial y^2}+\frac{\partial^2 \Psi_3}{\partial z^2}=0, \tag{B 29}$$

$$w_3\to 0 \quad \text{as } z\to -b, \tag{B 30}$$

$$h_{z_3}\to 0 \quad \text{as } z\to -b, \tag{B 31}$$

$$\frac{\partial \Psi_3}{\partial z}\to 0 \quad \text{as } z\to -b. \tag{B 32}$$

https://doi.org/10.1017/S0022377899008004 Published online by Cambridge University Press

References

Abdullaev, F. Kh. 1989 *Phys. Rep.* **179**, 1.

Ablowitz, M. J. and Clarkson, P. A. 1991 *Solitons, Nonlinear Evolution Equations and Inverse Scattering*. London Mathematical Society, Lecture Note Series 149. Cambridge University Press.

Byrd, P. F. and Friedman, M. D. 1971 *Handbook of Elliptic Integrals for Scientists and Engineers*. Springer-Verlag, New York.

Chandrasekhar, S. 1961 *Hydrodynamic and Hydromagnetic Stability*. Clarendon Press, Oxford.

Davey, A. and Stewartson, K. 1975 *Proc. R. Soc. Lond.* **A388**, 101.

Freeman, N. C. and Davey, A. 1975 *Proc. R. Soc. Lond.* **A344**, 427.

Grimshaw, R. and Tian, X. 1994 *Proc. R. Soc. Lond.* **A445**, 1.

Guckenheimer, P. and Holmes, P. J. 1983 *Nonlinear Oscillations, Dynamical Systems and Bifurcation of Vector Fields*. Springer-Verlag, New York.

Infeld, E. and Rowlands, G. 1988 *Phys. Rev. Lett.* **60**, 2273.

Jordan, D. W. and Smith, P. 1987 *Nonlinear Ordinary Differential Equations*. Clarendon Press, Oxford.

Kadomtsev, B. B. and Petviashvili, V. I. 1970 *J. Fluid Mech.* **15**, 539.

Malik, S. K. and Singh, M. 1989 *Phys. Rev. Lett.* **62**, 1753.

Malik, S. K. and Singh, M. 1991 *Magnit. Gidrodinam.* **4**, 17.

Melnikov, V. K. 1963 *Trans. Moscow Math. Soc.* **12**, 1.

Nayfeh, A. H. 1973 *Perturbation Methods*. Wiley, New York.

Ockendon, J. R. and Ockendon, H. 1973 *J. Fluid Mech.* **59**, 397.

Pusri, A. and Malik, S. K. 1995 *J. Plasma Phys.* **53**, 145.

Whitham, G. B. 1974 *Linear and Nonlinear Waves*. Wiley, New York.

https://doi.org/10.1017/S0022377899008004 Published online by Cambridge University Press